AAS 05-104

American Astronautical Society

American Institute of Aeronautics and Astronautics

STATIC EQUILIBRIUM CONFIGURATIONS IN GEO COULOMB SPACECRAFT FORMATIONS

John Berryman and Hanspeter Schaub

15th AAS/AIAA Space Flight Mechanics Meeting

Copper Mountain, CO Jan. 23–27, 2005

AAS Publications Office, P.O. Box 28130, San Diego, CA 92198

AAS 05-104

STATIC EQUILIBRIUM CONFIGURATIONS IN GEO COULOMB SPACECRAFT FORMATIONS

John Berryman* **and Hanspeter Schaub†**

The benefits of Coulomb control for spacecraft formations include minimal power usage, virtual lack of propellant, and low mass. Before this method of formation control is mission-worthy, the dynamics that govern the motion of charged spacecraft must be better understood. The purpose of this research is to use the evolutionary algorithm to numerically search for steady-state equilibriums in which the sum of the accelerations on each satellite is zero, essentially freezing the satellite formation with respect to the rotating Hill frame. Difficulties encountered will be discussed as well as methods to circumnavigate these difficulties.

1 INTRODUCTION

In recent years there has been increasing interest in close-proximity spacecraft formation flying. Here the spacecraft are flying tens to hundreds of meters apart with applications ranging from wide field of view sparse radar interferometry systems and autonomous robotic scouts flying about a mother craft, to swarms of pico-satellites that will provide a distributed sensing platform. King and Parker discuss in Reference 1 an attractive method of achieving a wide field of view interferometry mission using Coulomb thrusting. Using a distributed set of sensors, the discrete readings are combined to form a high-resolution image. Meter-level sensing accuracy with infinite dwell time could be achieved by having sensors flying tens of meters apart at geostationary altitudes to form a sparse interferometric dish. Building a single structure with diameter ranging from tens to hundreds of meters would be a very costly and challenging endeavor. Radar based interferometry, and especially optical interferometry, require very precise alignments of the sensors. Controlling the vibration and flexing modes of such large structures would be very daunting. Having discretely distributed sensors flying in a tight formation would provide an attractive alternative. Such formations would be more robust to single sensor failures. The formation could continue to function, even though it is operating at a reduced capacity.

Unfortunately, most close proximity missions are not feasible with the current technology available. Electric propulsion (EP) thrusters have been presented as a candidate technology for this task, however, they come with several problems that may ultimately prove insurmountable. The basic concept of the EP thruster is to rapidly accelerate and eject charged particles and in doing so propel the spacecraft forward. This method of propulsion has some beneficial qualities. For instance, the specific impulse provided by these systems tends to be very high, up to $I_{\rm sp}$ values of 6000 seconds. Additionally, the total mass of EP systems is often just a small fraction of the mass of more traditional propulsion systems.

*Graduate Student, Aerospace and Ocean Engineering Department, Virginia Tech, Blacksburg, VA 24061
†Assistant Professor, Virginia Tech, Blacksburg, VA 24061-0203.

Unfortunately, EP systems have one significant drawback: the charged particles that they emit are very caustic and tend to damage anything they contact. In most missions, this would be of no consequence because the propellant is discharged safely behind the spacecraft, but when several spacecraft are in close proximity to one another, the propellant can damage the payloads of neighboring crafts. Also, because EP expels particles to propel the spacecraft, the life of a mission will often be limited by the amount of propellant that can be carried aboard a spacecraft.[2]

In contrast to traditional formation flying concepts, King and Parker proposed in Reference 1 to control the relative spacecraft motion by exploiting the inter-spacecraft electrostatic (Coulomb) force. By raising and lowering the Coulomb charge of the spacecraft in a cluster, each spacecraft exerts a force on all other spacecraft. This force can potentially be exploited to control the shape, and thus the relative motion, of the spacecraft formation.[1–5] However, unlike EP systems, Coulomb control would be essentially propellantless with equivalent I_{sp} values to control the relative motion ranging up to 10^{10}–10^{13} seconds. Further, the electric power required to achieve this is often 1 Watt or less. The EP power requirements are typically orders of magnitude larger. Coulomb thrusting is a very clean method of relative motion propulsion and thus raises no problem of plume impingement with other spacecraft in a tight formation.[1,3] Due to the extremely high fuel-efficiency of these systems, they have been coined as being "essentially" propellantless. Finally, all relative motion is achieved using renewable electric energy.

Even though Coulomb control enjoys obvious advantages, it also has some drawbacks. This method of control is based upon the attraction and repulsion of charged bodies. For this reason, the charged plasma environment in space tends to diminish a spacecraft's influence upon other spacecraft by masking its charge. Additionally, the plasma environment of space tends to naturally charge a spacecraft. Significant spacecraft charging can be observed at altitudes as high as Geostationary Orbits (GEO).[6] With Coulomb control, all forces are internal, i.e., each satellite is either pushing or pulling against the others. For this reason, the inertial linear and rotational momentum can not be altered by Coulomb forces.[7,8] Finally, the dynamics of such a system are highly coupled and non-linear. For example, if the position or charge of one spacecraft is altered, then the forces on all formation spacecraft will be affected. Despite the difficulties involved with this approach of formation control, if the dynamics can be better understood, then the Coulomb control might one day be a fuel efficient, inexpensive, long lasting and dependable method for controlling close proximity formations.

Reference 2 discusses exciting static solutions of the charged spacecraft equations of motion. Here spacecraft charges are found which will cancel the orbital dynamics, yielding formations that are static as seen by the rotating Hill frame. Using formation symmetry and formation circular center of mass motion assumptions, analytical solutions are found for 3 to 7 spacecraft. These static formations are excellent candidate formations to develop virtual Coulomb structures. Here the craft are not orbiting about each other as in conventional spacecraft formation concepts; rather the Coulomb forces create an internal tension which allows the cluster to maintain a specific shape and act as a semi-rigid body. Substantial weight savings could be achieved if large GEO or deep-space structures could be built in this distributed manner.

The goal of this paper is to search for static Coulomb formations in circular orbits around a planet. The word *static* indicates that the positions of the formation spacecraft remain constant in the rotating Hill coordinate frame. This is achieved by positioning and charging the spacecraft so that the net accelerations due to attraction and repulsion of the spacecraft will cancel the accelerations in the Hill frame. References 2 and 3 have shown a few analytical results for simple geometries at GEO. This paper will extend this static Coulomb formation search by employing an Evolutionary Algorithm (EA) to numerically search for such formations.[9] Due to the fact that the system's equations of motion are highly nonlinear and coupled, static solutions are very non-intuitive and difficult to find – making this problem ideal for an EA. Of importance is that EA's require very little a priori knowledge of the solution. EA's have been used in complex space applications to search for low-thrust trajectories in References 10 and 11. Reference 12 developed an EA based station keeping strategy. This papers illustrates how an EA can be used to investigate the very complex and non-intuitive Coulomb formation dynamics. The results collected from the study will then be discussed. A final consideration will be given to the computational demands involved with the numerical search.

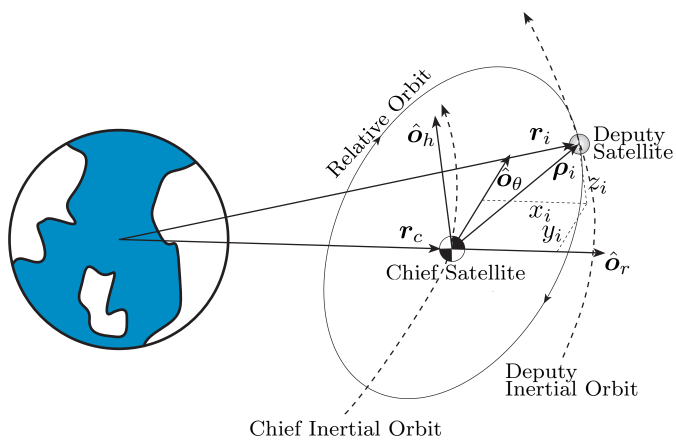

Figure 1: Illustration of the Rotating Hill Coordinate Frame

2 PROBLEM STATEMENT

Let $\boldsymbol{r}_i$ be the inertial position vector of a spacecraft, and $\boldsymbol{r}_c$ be the inertial formation center of mass position vector. The formation center of mass will be referred to as the chief position. As illustrated in Figure 1, the relative position vector is then defined as $\boldsymbol{\rho}_i = \boldsymbol{r}_i - \boldsymbol{r}_c$. The rotating Hill frame $\mathcal{H} : \{\hat{\boldsymbol{o}}_r, \hat{\boldsymbol{o}}_\theta, \hat{\boldsymbol{o}}_h\}$ is defined to follow the formation center of mass (or chief) motion. It has the unit orientation axis $\hat{\boldsymbol{o}}_r$ defined as the orbit radial direction of the formation center of mass position vector, $\hat{\boldsymbol{o}}_h$ pointing in the orbit normal direction, while $\hat{\boldsymbol{o}}_\theta$ completes the right handed triad. Let the ith relative position vector be expressed in Hill frame components as

$$\boldsymbol{\rho}_i = {}^{\mathcal{H}}\!\begin{pmatrix} x_i \\ y_i \\ z_i \end{pmatrix} \tag{1}$$

For a Coulomb formation to be static (or frozen) with respect to the Hill frame, then all relative motion velocity coordinates $(\dot{x}_i, \dot{y}_i, \dot{z}_i)$ and acceleration coordinates $(\ddot{x}_i, \ddot{y}_i, \ddot{z}_i)$ must be zero throughout the orbit. This is achieved through careful positioning and charging of the spacecraft such that the accelerations due to the charges exactly opposes the accelerations from the Hill frame, effectively nullifying one another. Mathematically, this can be seen by adding the Coulomb force terms to the right hand side of Hill's equations.[13–15]

$$\ddot{x}_i - 2n\dot{y}_i - 3n^2 x_i = \frac{k_c}{m_i} \sum_{j=1}^{N} \frac{x_i - x_j}{|\boldsymbol{\rho}_i - \boldsymbol{\rho}_j|^3} q_i q_j e^{-\frac{\lambda_d}{\rho_{ij}}} \tag{2}$$

$$\ddot{y}_i + 2n\dot{x}_i = \frac{k_c}{m_i} \sum_{j=1}^{N} \frac{y_i - y_j}{|\boldsymbol{\rho}_i - \boldsymbol{\rho}_j|^3} q_i q_j e^{-\frac{\lambda_d}{\rho_{ij}}} \tag{3}$$

$$\ddot{z}_i + n^2 z_i = \frac{k_c}{m_i} \sum_{j=1}^{N} \frac{z_i - z_j}{|\boldsymbol{\rho}_i - \boldsymbol{\rho}_j|^3} q_i q_j e^{-\frac{\lambda_d}{\rho_{ij}}} \tag{4}$$

The chief motion is assumed to be circular with a constant mean orbit rate n. The parameter $k_c = 8.99 \cdot 10^9$ Nm^2/C^2 is Coulomb's constant. When two charged bodies are brought near to one another, they exert a force on each other that is proportional to the product of their charges and inversely proportional to the square of the distance that separates them. Oppositely charged bodies will attract one another and similarly charged bodies will repel one another. The acceleration that is due to the force of one body on another is found by dividing the force by the mass of the body that is being accelerated. Therefore, the new terms on the right hand side of Hill's equations define the net acceleration experienced by one spacecraft due to its Coulomb interaction with all the other charged spacecraft. Note that the standard electrostatic inverse-square field strength formula is augmented with the exponential decay term. The Debye length λ_d determines how fast the field strength will weaken due to the interaction with the space plasma environment.[16–18] At GEO the Debye length is rather large with values ranging between 140–1400 meters. Because the static Coulomb formations considered only have dimensions of 10's of meters, the Debye length term is assumed to be infinitely large in this study.

Note that the Coulomb force term in Eqs. (2)–(4) couples the relative differential equations of motion of all spacecraft. This is in contrast to traditional formations where the motion of one craft does not directly influence the motion of other craft. This strong physical coupling makes searching for static steady-state Coulomb formations a non-trivial and non-intuitive matter.

To find static steady-state Coulomb formations, the spacecraft relative positions and charges are adjusted in these equations, such that the acceleration remains zero. Because we are searching for static solutions, the velocity coordinates $(\dot{x}_i, \dot{y}_i, \dot{z}_i)$ are set to zero. Without these Coulomb forces present, the only static solution of Hill's equations is the simple lead-follower formation where $x_i = z_i = 0$. If there is radial or out-of-plane relative motion, then the only bounded relative motion solutions will yield a 2:1 ellipse in the $(\hat{\boldsymbol{o}}_r, \hat{\boldsymbol{o}}_\theta)$ plane and a decoupled sinusoidal motion in the $\hat{\boldsymbol{o}}_h$ direction.[14,19]

3 STATIC COULOMB FORMATION SEARCH STRATEGY

As motivation for more complex cases involving many spacecraft, consider the simple case of two charged spacecraft of the same mass that are aligned along the radial axis. Because there will be no radial or along-track velocities, the equations decouple, and the following two equations are sufficient to determine the positions and charges of each spacecraft.

$$\ddot{x}_1 = 0 = \frac{k_c}{m}\frac{x_1 - x_2}{|\boldsymbol{\rho}_1 - \boldsymbol{\rho}_2|^3} q_1 q_2 + 3n^2 x_1 \tag{5}$$

$$\ddot{x}_2 = 0 = \frac{k_c}{m}\frac{x_2 - x_1}{|\boldsymbol{\rho}_2 - \boldsymbol{\rho}_1|^3} q_2 q_1 + 3n^2 x_2 \tag{6}$$

Note, the Debye length term is dropped here. Since both spacecraft are situated along the radial axis, the $|\boldsymbol{\rho}_1 - \boldsymbol{\rho}_2|^3$ term simplifies to $|x_1 - x_2|^3$, and the necessary conditions for a static formation become

$$\frac{k_c q_1 q_2}{m(x_1 - x_2)^2} = -3n^2 x_1 \tag{7}$$

$$\frac{k_c q_1 q_2}{m(x_1 - x_2)^2} = 3n^2 x_2 \tag{8}$$

By combining these two equations so that the quantity $k_c q_1 q_2 / m(x_1 - x_2)^2$ is eliminated, we find that the positions of the two crafts must be the same distance $d/2$ away from the origin of the Hill's frame. Thus $x_1 = -x_2 = d/2$ must be true for this simple static Coulomb solution, where d is the distance between the two crafts. The product of the two charges can be found by substituting this relationship into the first equation and then solving for the quantity $q_1 q_2$.

$$\frac{k_c q_1 q_2}{md^2} = -\frac{3}{2} n^2 d$$

$$q_1 q_2 = -\frac{3}{2}\frac{mn^2 d^3}{k_c} \tag{9}$$

As a more specific example, consider the following two spacecraft formation orbiting the Earth in a circular GEO orbit with $n = 7.2722 \times 10^{-5}\text{sec}^{-1}$. The spacecraft are both 100 kg and they are separated by 20 meters. If the spacecraft are charged to

$$q = \pm\sqrt{\frac{3}{2}\frac{mn^2 d^3}{k_c}} = \pm 8.4030 \times 10^{-7}\text{C}$$

then the above equations are satisfied. As long as no perturbations are present, this formation will remain stationary with respect to the Hill's frame.

With higher numbers of spacecraft that are arbitrarily positioned in the Hill's frame, the equations of motion become complicated, nonlinear, and highly coupled. Furthermore, with each additional spacecraft, there are three more equations that must be satisfied (i.e., Hill frame accelerations being zero for each new spacecraft), and four more unknowns (i.e., the elements of the position vector and the charge of each new spacecraft). Therefore, a direct analytical approach will be formidable for a large number of spacecraft making a numerical search for static Coulomb formations more appealing. Once several static formations are identified, new solutions can be analytically determined by reparameterizing the Hill's equations to reflect the resulting formations. Even solutions that are too complex to be useful in reparameterization can still provide a basic understanding of the possibilities of static Coulomb formations.

The problem can be extended to N spacecraft by considering the additional free parameters attributed to each new spacecraft. For the case of two spacecraft, the free parameters are the positions and the charges of each spacecraft. This is also true for the general case except that the position of each spacecraft now has three free parameters instead of one. So for Coulomb formations with N spacecraft there are $4N$ parameters which must be determined: the 3 directional coordinates for each spacecraft and the charge for each spacecraft. This total number of parameters can be reduced by 3 by defining the center of mass of the formation to coincide with the origin of the Hill frame. Here the relative position vectors must satisfy

$$\sum_{i=1}^{N} m_i x_i = \sum_{i=1}^{N} m_i y_i = \sum_{i=1}^{N} m_i z_i = 0 \tag{10}$$

So the final number of parameters for N spacecraft is $4N - 3$. Applying this constraint on the position coordinates, (x_i, y_i, z_i), eliminates repeated solutions, (i.e., solutions that are identical but are displaced by a constant distance in the along track direction). It is still possible to find solutions with identical configurations that are oriented differently. In fact, finding such shapes that can exist with arbitrary orientations would be of great interest.

4 EVOLUTIONARY ALGORITHM

4.1 Search Algorithm Outline

Let $\boldsymbol{p}$ represent a parameter vector containing

$$\boldsymbol{p} = (x_1, y_1, z_1, q_1, \cdots, x_{N-1}, y_{N-1}, z_{N-1}, q_{N-1}, q_N) \tag{11}$$

Note that these parameters do not contain the (x_N, y_N, z_N) coordinates. These are found by employing the formation center of mass constraint

$$\boldsymbol{\rho}_N = {}^{\mathcal{H}}\!\begin{pmatrix} x_N \\ y_N \\ z_N \end{pmatrix} = \frac{1}{M} \sum_{i=1}^{N-1} m_i \boldsymbol{\rho}_i \tag{12}$$

where

$$M = \sum_{i=1}^{N} m_i \tag{13}$$

is the total formation mass. To simplify this study, the mass of each spacecraft is chosen to be 1kg. To find the static Coulomb formations, a cost function $J(\boldsymbol{p})$ is defined to be a

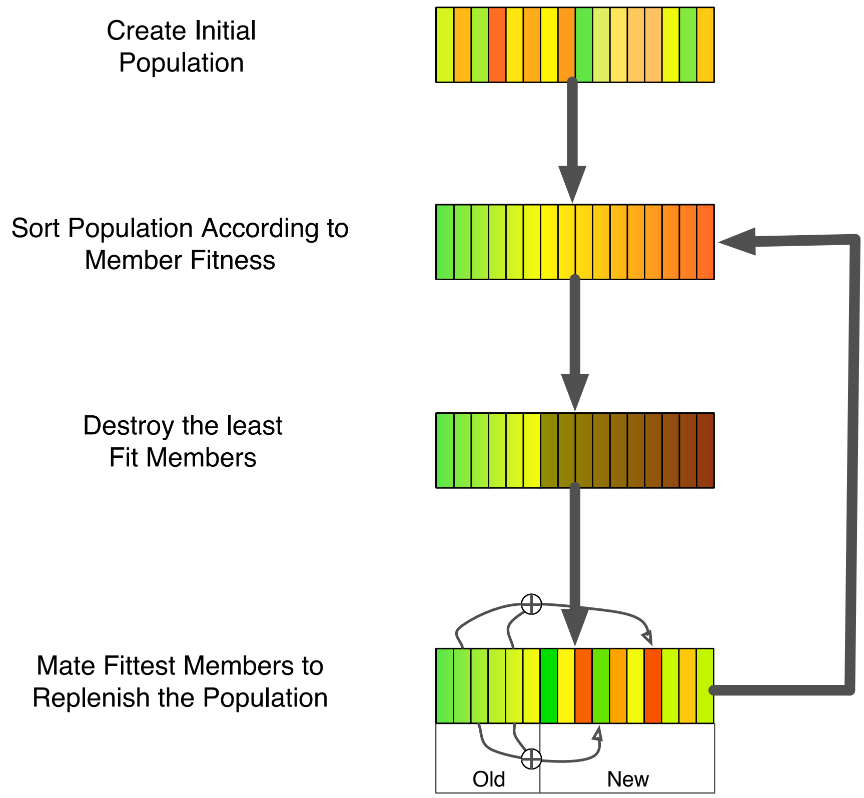

Figure 2: Illustration of the Single-Processor Evolutionary Algorithm

positive definite measure of the spacecraft accelerations $(\ddot{x}_i, \ddot{y}_i, \ddot{z}_i)$. If $J(\boldsymbol{p}) = 0$, then a set of parameters has been found which yields a static Coulomb formation. An obvious numerical algorithm to minimize $J(\boldsymbol{p})$ is a gradient based numerical optimization scheme. Using an initial guess of $\boldsymbol{p}$, the numerical optimizer proceeds in the direction of steepest decent $\partial J/\partial \boldsymbol{p}$ until finally coming to rest when the cost function evaluates to zero, indicating that the spacecraft are fixed relative to the Hill's frame. Unfortunately, in practice, it is not this simple. Gradient based methods require that an initial guess be given. However, for the problem at hand, there are few obvious initial guesses. Furthermore, the gradient based methods will only search for solutions in the neighborhood of the initial guesses. Since the equations involved here are non-intuitive by nature, there are likely many solutions scattered throughout the search space. Searching in the neighborhood of a few carefully selected initial guesses would prevent the less intuitive solutions from being discovered. For these reasons, gradient based methods are less preferable for the problem discussed here.

Evolutionary algorithms (EA) are a relatively new group of methods used to solve a wide range of problems. The evolutionary algorithm employed in this study is outlined in Figure 2. Initially, a population is created where each member is a set of parameters $\boldsymbol{p}$ that describes a potential solution. The members of this initial population are scattered throughout the search space. For N spacecraft, each set of parameters would contain N values that define the charge of each spacecraft and $3N-3$ values that define their positions. The EA then "mates" the members of this initial population so that their offspring represent a recombination of the parent's parameters.

Often the parameters are represented in binary form and then concatenated as a single string of ones and zeros. The algorithm used in this study did not concatenate the parameters. Rather, it kept each parameter a separate entity represented by a double precision number. To mate two parents together, the algorithm used one of two methods. The first method is to create a child whose parameters are randomly chosen from the parameters of the parents. For instance, the charge of spacecraft 1 might come from the mother while the charge of spacecraft 2 could be from the father. The mating of an individual parameter value by this method can be displayed algebraically.

$$p_{i_{\text{child}}} = (r_{i_{\text{bit}}}) \times p_{i_{\text{mother}}} + (!r_{i_{\text{bit}}}) \times p_{i_{\text{father}}} \tag{14}$$

Where $r_{i_{\text{bit}}}$ is a random number that is either 0 or 1 and p_i represents a generic parameter. To mate the entire parameter vector $\boldsymbol{p}$ this equation is used for each individual parameter value.

The second mating method involved interpolating to some arbitrary point around the parents. For instance the child could receive 40% of it's spacecraft 1 charge from the mother and 60% from the father, (a weighted average of the two charges), and the charge for spacecraft 2 could be a different weighted average of the parents parameters. The second method is extended to allow the algorithm to search in areas slightly outside of the area between the parents. This was done by allowing the weighted average to go beyond a 0%/100% ratio. In the extreme case, it would be possible for a child to receive 125% of a parameter value from one parent while receiving -25% from the other.

$$p_{i_{\text{child}}} = (r_{\text{rand}}) \times p_{i_{\text{mother}}} + (1 - r_{\text{rand}}) \times p_{i_{\text{father}}} \tag{15}$$

The parameter r_{rand} is a random number of binomial distribution that is between -0.25 and 1.25. During a search for a formation, the algorithm randomly executes both methods of mating in equal proportions.

Parameter mutation is also included to increase variability and explore new portions of the parameter space. This is done by adding a random number, r_{mutation}, to a child's current parameter value. This number is generated by taking the product of a random number of a Gaussian distribution, the maximum allowable value of the parameter being mutated and a term that oscillates periodically as a function of generation. (The Gaussian random number has a mean of 0, and a standard deviation and variance of 1.) Let q be an EA parameter that is to be mutated. The total mutation for a charge can be algebraically represented as

$$q_{\text{mutated}} = q_{\text{original}} + r_{\text{mutation}} \tag{16}$$

where

$$r_{\text{mutation}} = r_{\text{gaussian}}\, q_{\text{max}} \left(\cos\left(\frac{\text{generation}}{3} \right) + 1 \right)^2 \tag{17}$$

The last term, a periodic function of generation, is present so that during some generations the mutation will be large, and during other generations the mutation will be small. This allows the mutation to at times search randomly in distant territory of the cost domain and at other times to zero in on the current best solution(s).

With each successive generation, only the most "fit" members are allowed to procreate thereby improving population fitness until the members converge to a single point in the search space. Ideal fitness for a Coulomb formation occurs when the net acceleration of each spacecraft is zero, or at least as close as machine precision allows. There are several variations of the EA, but all of them in some manner use this Darwinian approach to improve member fitness and find a solution. Although the EA, as outlined above, describes an algorithm that would be used on a single-processor, this basic idea can be easily extended for use in a distributed computing platform making it an even more powerful tool for optimization.

This approach to optimization offers several advantages over some of the more traditional, gradient based methods. Most notably, the EA does not require an initial guess, but only a domain in which to search. Also, the very nature of EAs allow them to search the parameter space in a much more global manner than a gradient based method. While gradient based algorithms search in the neighborhood of an initial guess, EA's use many different initial guesses. By recombining and mutating their parameters, each member of a population shares information with the others, looks in places that might not be obvious, and in effect cooperates in searching for a more global solution. Finally, EA's are generally more equipped for solving unconventional problems than the more traditional methods. For instance, EAs are capable of handling problems with both continuous and discreet parameters just as easily as it would handle a problem with only continuous parameters. Despite these advantages, EA's are computationally intensive, and in circumstances where the problem is linear and well behaved, it is generally better to use a gradient based method. However, determination of static Coulomb formations involves highly coupled nonlinear equations, making the EA an attractive computational tool to explore static formation solutions.

4.2 Cost Function Definition

To numerically search for static Coulomb formations, cost function $J(\boldsymbol{p})$ is defined which is a positive definite measure of the spacecraft accelerations in the Hill frame. As the accelerations of the spacecraft decrease, $J(\boldsymbol{p})$ will also decrease. In the limiting case, each spacecraft will have no acceleration and $J(\boldsymbol{p})$ will be identically 0. The following discussion explores several cost functions and strategies that were used during this research. First, some of the terms used in the cost function must be clearly defined. Let the acceleration components in the Hill frame be expressed as

$$a_{x_i} = \frac{k_c}{m_i} \sum_{j=1}^{N} \frac{x_i - x_j}{|\boldsymbol{\rho}_i - \boldsymbol{\rho}_j|^3} q_i q_j + 3n^2 x_i \tag{18}$$

$$a_{y_i} = \frac{k_c}{m_i} \sum_{j=1}^{N} \frac{y_i - y_j}{|\boldsymbol{\rho}_i - \boldsymbol{\rho}_j|^3} q_i q_j \tag{19}$$

$$a_{z_i} = \frac{k_c}{m_i} \sum_{j=1}^{N} \frac{z_i - z_j}{|\boldsymbol{\rho}_i - \boldsymbol{\rho}_j|^3} q_i q_j - n^2 z_i \tag{20}$$

Note that for static, steady-state solutions these accelerations must remain zero. Here all coordinate rates $\dot{x}_i$, $\dot{y}_i$ and $\dot{z}_i$ are set to zero. The acceleration vector that would result if all N craft were placed at (x_i, y_i, z_i) with zero velocity is

$$\boldsymbol{a}_i = {}^{\mathcal{H}}\!\begin{pmatrix} a_{x_i} \\ a_{y_i} \\ a_{z_i} \end{pmatrix} \tag{21}$$

Also $\boldsymbol{a}_{ij}$ represents the acceleration imparted to spacecraft i by its Coulomb force field interaction with spacecraft j. This is algebraically represented as

$$\boldsymbol{a}_{ij} = \frac{k_c}{m_i} \frac{\boldsymbol{\rho}_i - \boldsymbol{\rho}_j}{|\boldsymbol{\rho}_i - \boldsymbol{\rho}_j|^3} q_i q_j \tag{22}$$

The following cost function was first considered for determining Coulomb formations.

$$J(\boldsymbol{p}) = \sum_{i=1}^{N} \|\boldsymbol{a}_i\| \tag{23}$$

Literally, this function is minimized as the sum of the acceleration magnitudes approaches zero. This cost function seems to be the most obvious; however in practice, it almost always leads to a trivial solution. As $J(\boldsymbol{p})$ approaches zero, the charges for all or all but one of the spacecraft move toward zero and each spacecraft becomes aligned with the $\hat{\boldsymbol{o}}_\theta$ along-track axis. When the charges are set to zero, there is obviously no inter-spacecraft acceleration due to the Coulomb charge. Furthermore, when the spacecraft are aligned along the $\hat{\boldsymbol{o}}_\theta$ axis in a classical lead-follower formation, the Hill frame accelerations vanish as well. Therefore, even though this is a solution, it is of little interest because they do not exploit the spacecraft charging properties. Thus the algorithm or the cost function must be altered in order to avoid this trivial charge-free case.

The first modification to the search algorithm quarantined members of the EA population as a means of avoiding this trivial solution. Lower magnitude bounds were imposed on the spacecraft charges. Each time one of the charges became smaller than a lower bound, the charge would be reset. The effect was similar to a mutation; therefore the member was still useful in searching the space, while remaining at a distance from the trivial solution. Unfortunately, this method was completely ineffective. Once the EA was forced to search outside the trivial solution, the results often converged to non-optimal points along the constraint boundary.

Finally, a weighting term was included in the cost function that effectively avoided the trivial solution. A new cost function was created by dividing the previous one by the sum of the magnitudes of the inter-spacecraft accelerations, as seen here:

$$J(\boldsymbol{p}) = \sum_{i=1}^{N} \|\boldsymbol{a}_i\| \Bigg/ \sum_{j=1}^{N} \sum_{i=1}^{N} \|\boldsymbol{a}_{ij}\| \tag{24}$$

This cost function not only measures the net accelerations of each spacecraft, but now the denominator provides a measure of the Coulomb interaction between the spacecraft.

Therefore, as the trivial solution is approached – as the Coulomb interaction becomes very weak – the denominator approaches zero and the cost increases, effectively masking the trivial solution. However, the non-trivial solutions – those formations that are static and who's inter-spacecraft interactions are non-negligible – will still have a cost of zero.

This cost function effectively removes the trivial solution from the search space such that each successful run of the EA produces a new, nontrivial solution. In addition, because it reflects the strength of the spacecraft interactions, the new term provides an unexpected benefit by causing the EA to be more attracted to static formations with stronger Coulomb interaction. Therefore, if a resulting formation is being used as a virtual structure, the interaction between spacecraft will cause it to behave more like a rigid body.

Nevertheless, there are drawbacks to this cost function. With the inclusion of the new term, the topology of the fitness function becomes more complicated. The absolute value in the denominator leads to cusps and troughs located sporadically throughout the search space that previously did not exist. Additionally, the new cost function does not allow the EA to easily find the formations that, although less rigid, might still be of value.

Another problem encountered involves machine precision. The cost function $J(\boldsymbol{p})$ as stated contains large terms such as $k_c = 8.9876 \times 10^9 \mathrm{Nm}^2\mathrm{C}^{-2}$ and small terms such as charges that might be as small as fractions of μC. Because of this mixture of extremely large and small terms, the results of the mathematical operations can be near machine precision. By normalizing the charge with respect to the Coulomb constant k_c and the mean orbit rate n, the Hill frame accelerations can be reparameterized as follows.

$$\tilde{a}_{x_i} = \frac{1}{m_i} \sum_{j=1}^{N} \frac{x_i - x_j}{|\boldsymbol{\rho}_i - \boldsymbol{\rho}_j|^3} \tilde{q}_i \tilde{q}_j + 3x_i \tag{25}$$

$$\tilde{a}_{y_i} = \frac{1}{m_i} \sum_{j=1}^{N} \frac{y_i - y_j}{|\boldsymbol{\rho}_i - \boldsymbol{\rho}_j|^3} \tilde{q}_i \tilde{q}_j \tag{26}$$

$$\tilde{a}_{z_i} = \frac{1}{m_i} \sum_{j=1}^{N} \frac{z_i - z_j}{|\boldsymbol{\rho}_i - \boldsymbol{\rho}_j|^3} \tilde{q}_i \tilde{q}_j - z_i \tag{27}$$

where $i \neq j$, $\tilde{q}_i = q_i\sqrt{k_c}/n$ and $\tilde{\boldsymbol{a}}_i = \boldsymbol{a}_i/n^2$. With this reparameterization, all of the terms computed are on the order of 100 for formations up to 50 meters in diameter. Also, because the mean orbit rate n is no longer present in any of the equations, the solutions are applicable to a circular orbit of any radius. This assumes that the local Debye length is large enough that the exponential terms in equations 2-4 are negligible.

5 GEO STATIC COULOMB FORMATION SOLUTIONS

The following are examples of various static Coulomb formations in the Hill frame. The criteria for considering a formation "static" in the Hill frame is that the average acceleration magnitude of the spacecraft must be a small fraction of the typical Hill acceleration that a spacecraft might experience. Figure 3(a) displays a typical two-spacecraft formation. As demonstrated in the earlier example, all two-spacecraft formations must be aligned along the $\hat{\boldsymbol{o}}_r$ axis for the equations to decouple and for a solution to be possible. Any off-axis tilt seen in the figure can be attributed to incomplete convergence of the EA. If the criteria for convergence is made more stringent, then the tilt would be less apparent; however. it would be much more time consuming to find a solution. These simple formations might be useful as virtual tethers between two spacecraft. Note that a two-spacecraft formation is only possible in the rotating Hill frame. In free space, non-zero charges would always cause the crafts to either attract or repel one another and the formation could not remain static.

Figures 3(b)–3(e) show various Coulomb formations that were determined for three spacecraft. There are two linear formations, one aligned with the $\hat{\boldsymbol{o}}_h$ axis, Figure 3(b), and one aligned with the $\hat{\boldsymbol{o}}_\theta$ axis, Figure 3(c). These collinear three-satellite static Coulomb formations have been shown to exist analytically by King and Parker.[1,2] Like the two-spacecraft formations, these formations could also be useful as virtual Coulomb tethers, perhaps even more so because the magnitude of the inter-craft accelerations, $(\sum_j \sum_i \|\boldsymbol{a}_{ij}\|)$, appears to be up to seven times stronger than that of the two-spacecraft formations.

Figure 3(d) displays a triangular formation that is perpendicular to the $\hat{\boldsymbol{o}}_\theta$ axis. A solution was also found that is perpendicular to the $\hat{\boldsymbol{o}}_h$ axis, (Figure 3(e)). Similar formations have been analytically determined in Reference 3. However, these are constrained to be symmetric about the $\hat{\boldsymbol{o}}_r$ axis, whereas the formations determined by the EA did not require symmetry. This indicates that a larger class of triangular formations exists than previously considered.

Figures 4(a) – 4(d) illustrate static Coulomb formation solutions for higher number of satellites. The formations continue to become more complex with each additional spacecraft. Most of the four-spacecraft formations were shallow, nearly planar pyramids. The five-spacecraft formations had several different forms, from nearly planar quadrilateral formations with an oppositely charged spacecraft in the center, to formations that appeared reminiscent of the spacecraft from the classic Atari game, *Asteroids*. With five-spacecraft formations, some patterns began to appear. For instance, there is a tendency toward geometric symmetry about the plane perpendicular to the $\hat{\boldsymbol{o}}_h$ axis as seen in figure 4(a). Also, there appears to be a balance of charge about the plane perpendicular to the $\hat{\boldsymbol{o}}_r$ axis. If there is a group of positively charged spacecraft on one side of this plane, then there will often be a corresponding negative group on the opposite side, figure 4(b). This becomes more difficult to observe with an increased number of spacecraft. As the number is increased to ten and eleven spacecraft, the formations, while retaining some sense of symmetry, tended to appear more disorganized. This indicates that with an increased number of satellites, it becomes easier to satisfy the static Coulomb formation constraints, and thus the satellites can be placed at in more general ways.

Several of the satellite formations possess interesting traits worth investigating. For example, figure 4(c) shows a planar ring of negatively charged spacecraft with a positively charged spacecraft at a position near the center of this ring. This resembles a sparse aperture telescope with a circular array of five collectors and a combiner in the center. If this formation is an example of a larger family of formations then it could possibly be reconfigured for optimal interferometry requirements. Additionally, this formation provides hope that similar formations could be constructed with even more spacecraft. The nine-spacecraft formation in figure 4(d) is interesting because its spacecraft form two orthogonal planes alined with the Hill axes, and besides the rogue spacecraft to the side of the formation, everything appears to be fairly symmetrical. There are many more interesting formations, most of which again resemble a space fighter from an arcade game. These could potential

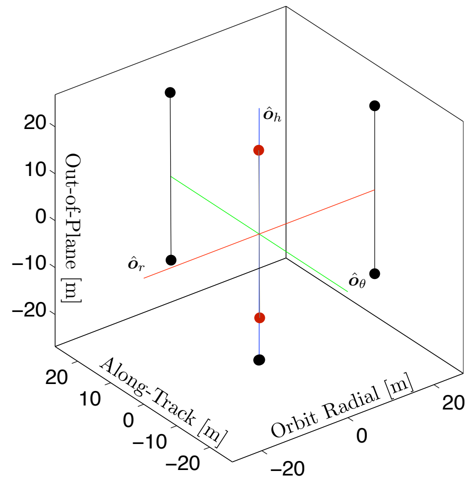

(a) Two Spacecraft Formation

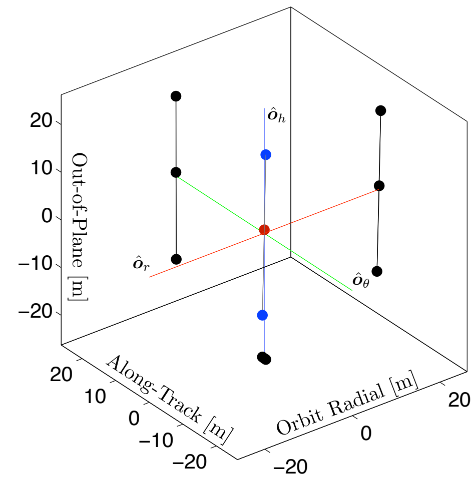

(b) $\hat{\boldsymbol{o}}_h$ Aligned Three Spacecraft Formation

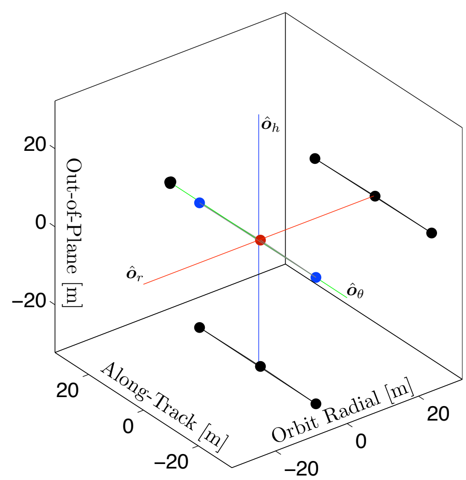

(c) $\hat{\boldsymbol{o}}_\theta$ Aligned Three Spacecraft Formation

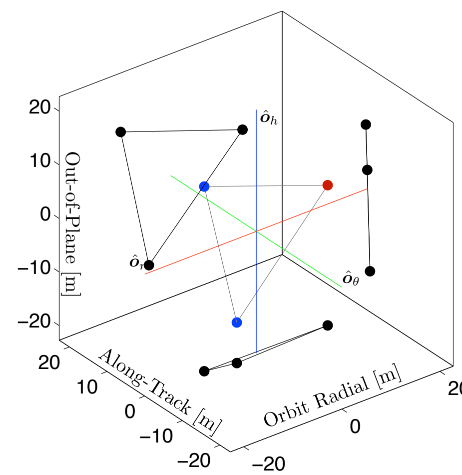

(d) $\hat{\boldsymbol{o}}_\theta$ Perpendicular Triangular Spacecraft Formation

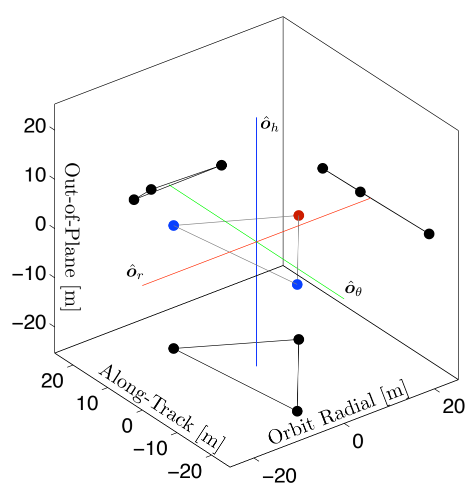

(e) $\hat{\boldsymbol{o}}_h$ Perpendicular Triangular Spacecraft Formation

Figure 3: Examples of two and three spacecraft formation that were determined by the EA.

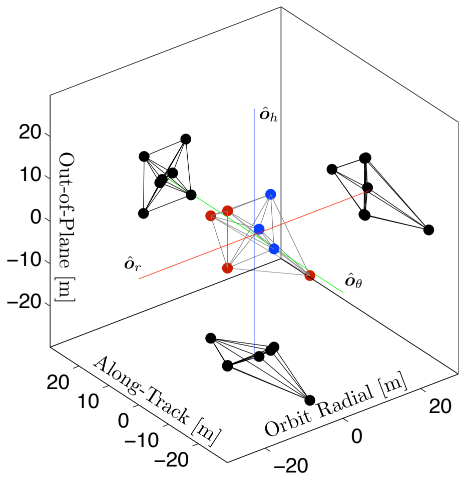

(a) Seven Spacecraft Formation

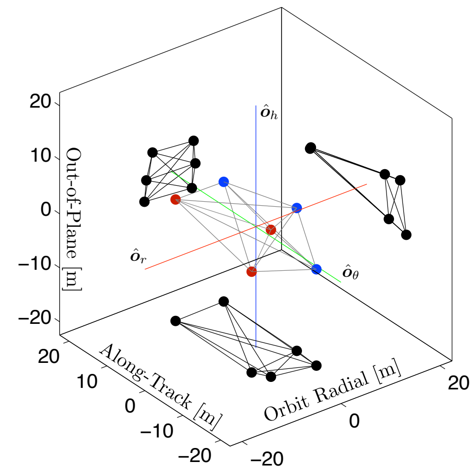

(b) Six Spacecraft Formation (Balanced Charges)

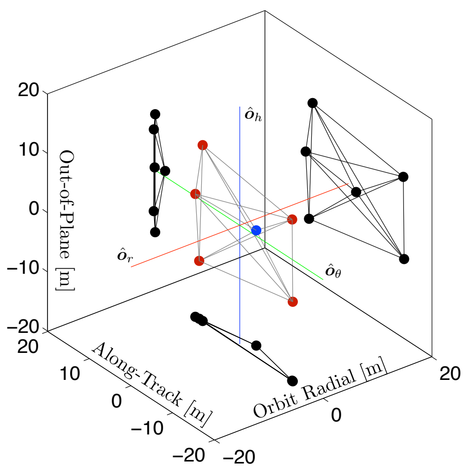

(c) Six Spacecraft Formation (Potential as Sparse Aperture)

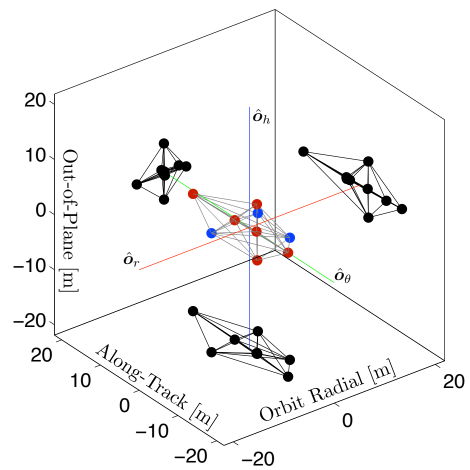

(d) Nine Spacecraft Formation

Figure 4: Examples of six, seven, and nine spacecraft formation that were determined by the EA.

be used as models for virtual structures.

A final consideration is given to the amount of computation necessary to find an N-spacecraft formation using the EA. Figure 5 displays the average number of generations that are necessary to find a formation with N spacecraft. In this study, the EA evaluates 200 new parameter sets, $\boldsymbol{p}$, per generation. Notice that the computational effort grows exponentially with the number of spacecraft included in a formation. Also notice that there is an unexpected increase in the computational effort required for nine spacecraft. Since the EA only recorded ten formations per each number of spacecraft, the sample size was small, and the increase could be due to a single run of the EA that was abnormally time consuming. Another possibility is that it might simply be more difficult to adequately adjust the charges and positions of nine crafts so that a static formation is achieved. No matter the

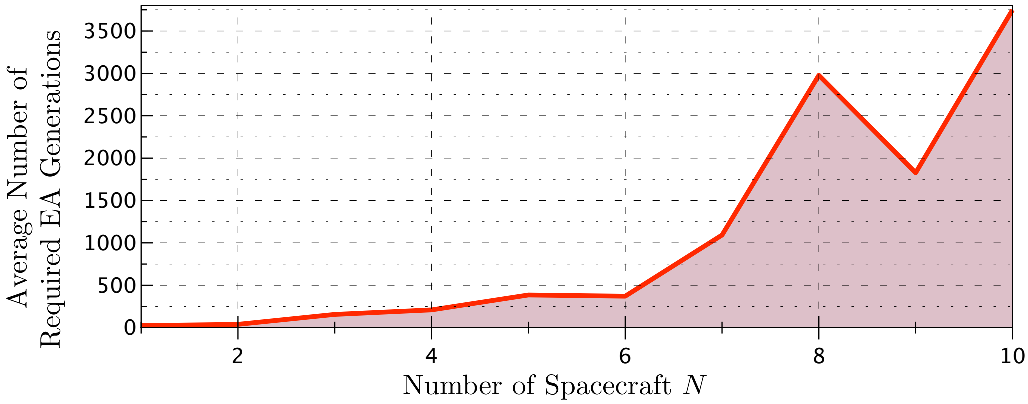

Figure 5: Computation necessary to realize an N spacecraft formation using the EA

case, the general trend is still an exponential increase with the number of spacecraft in the formation. If large numbers of spacecraft are to be considered, then computational power must be greatly increased before a numerical analysis will be possible. This is especially true if dynamic, repeating Coulomb spacecraft formations are to be investigated.

6 CONCLUSIONS

Coulomb controlled formations offers an alternative to other candidate propulsion systems because weigh less and are more fuel efficient. Additionally, Coulomb control is essentially propellantless and is therefore much less likely to damage formation spacecraft due to plume impingement. If sufficiently developed, this technology could provide a reliable and inexpensive method of formation control. The various examples of Hill frame static formations presented here serve to further encourage the study of Coulomb interaction as a means of controlling close proximity spacecraft formations. Formations similar to these could be used for various purposes from sparse aperture telescopes to virtual space structures and Coulomb tethers.

Although these results are encouraging, much work is needed before this technology is feasible for actual space application. The formations demonstrated in this paper are considered to be static, however there is no guarantee that they are stable or even controllable. A slight perturbation could conceivable send the spacecraft irretrievably into space. Therefore future research is essential to demonstrate both the stability and/or controllability of these formations.

Future research will consider dynamic formations that are periodic in nature and expanding the EA to take advantage of parallel processing. Although the formations currently considered are all static in the Hill frame, it should be possible to have moving formations with patterns that repeat periodically. As the research moves from static to dynamic formations and to an increased number of spacecraft, the computational requirements will greatly increase. Expanding the EA to a distributed computing platform will help accommodate the demands of future research.

A STATIC COULOMB FORMATION DATA

This appendix lists the spacecraft formation data that yielded the discussed static Coulomb formation solutions. Table 1 contains the data that produced Figures 3 and 4. The (x_i, y_i, z_i) coordinates of each craft are taken in the rotating Hill frame $\mathcal{H}$.

Table 1: Static Coulomb Formation with N Satellites.

Description	Sat No.	x_i [m]	y_i [m]	z_i [m]	$\tilde{q}_i$ $[C\frac{\sqrt{k_c}}{n}]$
2 Spacecraft	1	-0.092664	0.011066	17.8917	166.7136
Formation	2	0.092664	-0.011066	-17.8917	136.896
3 Spacecraft Linear	1	-0.023484	-0.075065	0.7652	37.4897
Formation ($\hat{\boldsymbol{o}}_h$ aligned)	2	-0.024972	-0.51724	16.7249	-206.2658
	3	0.048456	0.59231	-17.4901	-266.0775
3 Spacecraft Linear	1	-0.036273	21.4974	-0.26514	-175.3544
Formation ($\hat{\boldsymbol{o}}_\theta$ aligned)	2	0.18339	-0.41802	0.11892	42.0475
	3	-0.14712	-21.0794	0.14622	-161.5587
3 Spacecraft Triangular	1	-4.4331	-0.60236	-15.151	-77.022
Formation	2	14.6396	0.1004	3.4265	109.706
(Perpendicular to $\hat{\boldsymbol{o}}_\theta$)	3	-10.2065	0.50196	11.7245	-237.0545
3 Spacecraft Triangular	1	11.6585	3.0029	-0.12805	105.9299
Formation	2	-7.7367	13.8648	-0.30896	-128.7732
(Perpendicular to $\hat{\boldsymbol{o}}_h$)	3	-3.9218	-16.8678	0.43701	-101.1125
7 Spacecraft	1	5.2046	1.2553	7.1177	-34.5258
Formation	2	-0.8901	-19.8049	-0.26195	34.5104
	3	-1.4872	12.6487	-0.82082	13.4644
	4	-5.6985	1.5323	-6.5856	40.5746
	5	1.8194	0.7205	0.31747	-3.997
	6	-5.5185	1.7321	6.7684	40.3356
	7	6.5702	1.916	-6.5351	-54.7031
6 Spacecraft	1	-3.6757	-8.7775	4.7316	18.6585
Formation	2	-4.9418	14.7365	0.032367	31.8215
	3	4.9927	14.9707	-0.31142	-41.7238
	4	-5.3036	-5.8118	-3.7998	39.6514
	5	4.2763	-10.394	-4.6351	-30.5965
	6	4.6521	-4.7239	3.9824	-34.3029
6 Spacecraft	1	-0.30092	10.2766	0.69744	26.2459
Formation	2	-0.44629	-13.1755	7.1652	42.4876
	3	1.6249	-1.8444	-0.5891	-30.4786
	4	-0.19733	9.4761	-10.2863	43.6042
	5	-0.47352	-13.3682	-6.6336	42.4052
	6	-0.20681	8.6353	9.6464	24.5486
9 Spacecraft	1	-5.5614	2.5774	-0.27129	-22.9893
Formation	2	4.235	3.3704	-0.42808	-17.4779
	3	-0.27082	3.4834	-0.18405	9.2982

Continued on next page

Table 1 – continued from previous page

Description	Sat No.	x_i [m]	y_i [m]	z_i [m]	$\tilde{q}_i$ [$C\frac{\sqrt{k_c}}{n}$]
	4	-0.1535	-2.1963	-4.9073	24.1564
	5	-0.68204	-10.8544	0.61756	18.562
	6	-0.13938	-1.986	0.21305	4.536
	7	2.7537	-6.8262	0.27898	-11.1816
	8	-0.0029009	14.5789	-0.58875	70.537
	9	-0.17873	-2.1472	5.2699	21.4357

REFERENCES

[1] King, Lyon B., Parker, Gordon G., Deshmukh, Satwik, et al., "Spacecraft Formation-Flying using Inter-Vehicle Coulomb Forces", Tech. rep., NASA/NIAC, January 2002, `http://www.niac.usra.edu`.

[2] King, Lyon B., Parker, Gordon G., Deshmukh, Satwik, et al., "Study of Interspacecraft Coulomb Forces and Implications for Formation Flying", *AIAA Journal of Propulsion and Power*, Vol. 19, No. 3, May–June 2003, pp. 497–505.

[3] Schaub, Hanspeter, Parker, Gordon G., and King, Lyon B., "Challenges and Prospect of Coulomb Formations", *AAS John L. Junkins Astrodynamics Symposium*, College Station, TX, May 23-24 2003, Paper No. AAS-03-278.

[4] Chong, Jer-Hong, *Dynamic Behavior of Spacecraft Formation Flying using Coulomb Forces*, Master's thesis, Michigan Technological University, May 2002.

[5] Schaub, Hanspeter, "Stabilization of Satellite Motion Relative to a Coulomb Spacecraft Formation", *AAS Space Flight Mechanics Meeting*, Maui, Hawaii, Feb. 8–12 2004.

[6] Mullen, E. G., Gussenhoven, M. S., and Hardy, D. A, "SCATHA Survey of High-Voltage Spacecraft Charging in Sunlight", *Journal of the Geophysical Sciences*, Vol. 91, 1986, pp. 1074–1090.

[7] Schaub, Hanspeter and Parker, Gordon G., "Constraints of Coulomb Satellite Formation Dynamics: Part I – Cartesian Coordinates", *Journal of Celestial Mechanics and Dynamical Astronomy*, 2004, submitted for publication.

[8] Schaub, Hanspeter and Kim, Mischa, "Orbit Element Difference Constraints for Coulomb Satellite Formations", *AIAA/AAS Astrodynamics Specialist Conference*, Providence, Rhode Island, Aug. 2004, paper No. AIAA 04-5213.

[9] Goldberg, D. E., *Genetic Algorithms in Search, Optimization & Machine Learning*, Addison-Wesley Publishing Company, Inc., 1989.

[10] Hartmann, J. W., Coverstone-Carroll, Victoria, and Williams, S. N., "Generation of Optimal Spacecraft Trajectories via a Pareto Genetic Algorithm", *Journal of the Astronautical Sciences*, Vol. 46, No. 3, 1998, pp. 267–282.

[11] Coverstone-Carroll, Victoria, "Near-Optimal Low-Thrust Trajectories Via Micro-Genetic Algorithms", *Journal of Guidance, Control, and Dynamics*, Vol. 20, No. 1, 1997, pp. 196–198.

[12] Smith, J., Proulx, Ronald J., Cefola, Paul, et al., "Optimal Station Keeping Strategies via Parallel Genetic Algorithms", *AAS/AIAA Spaceflight Mechanics Meeting*, 1999, (pp. 303–321).

[13] Clohessy, W. H. and Wiltshire, R. S., "Terminal Guidance System for Satellite Rendezvous", *Journal of the Aerospace Sciences*, Vol. 27, No. 9, Sept. 1960, pp. 653–658.

[14] Schaub, Hanspeter and Junkins, John L., *Analytical Mechanics of Space Systems*, AIAA Education Series, Reston, VA, October 2003.

[15] Hill, George William, "Researches in the Lunar Theory", *American Journal of Mathematics*, Vol. 1, No. 1, 1878, pp. 5–26.

[16] Nicholson, Dwight R., *Introduction to Plasma Theory*, Krieger, 1992.

[17] Garrett, H. B., Schwank, D. C., and DeFrost, S. E., "A Statistical Analysis of the Low Energy Geosynchronous Plasma Environment. -I Protons", *Planetary Space Science*, Vol. 29, 1981b, pp. 1045–1060.

[18] Garrett, H. B., Schwank, D. C., and DeFrost, S. E., "A Statistical Analysis of the Low Energy Geosynchronous Plasma Environment. -I Electrons", *Planetary Space Science*, Vol. 29, 1981a, pp. 1021–1044.

[19] Schaub, Hanspeter, "Relative Orbit Geometry Through Classical Orbit Element Differences", *Journal of Guidance, Control and Dynamics*, Vol. 27, No. 5, Sept.–Oct. 2004, pp. 839–848.